HAL
open science

Dependence of the final state of the magnetization in ferromagnetic bilayers on the magnitude of the super-exchange energy

Stéphane Labbé, Kévin Santugini-Repiquet

To cite this version:

Stéphane Labbé, Kévin Santugini-Repiquet. Dependence of the final state of the magnetization in ferromagnetic bilayers on the magnitude of the super-exchange energy. 2012. hal-00676405

HAL Id: hal-00676405

https://hal.science/hal-00676405v1

Preprint submitted on 5 Mar 2012

HAL is a multi-disciplinary open access archive for the deposit and dissemination of scientific research documents, whether they are published or not. The documents may come from teaching and research institutions in France or abroad, or from public or private research centers.

L'archive ouverte pluridisciplinaire **HAL**, est destinée au dépôt et à la diffusion de documents scientifiques de niveau recherche, publiés ou non, émanant des établissements d'enseignement et de recherche français ou étrangers, des laboratoires publics ou privés.

Dependence of the final state of the magnetization in ferromagnetic bilayers on the magnitude of the super-exchange energy

Stéphane Labbé*, Kévin Santugini†

February 26, 2012

Abstract

We study the magnetic behavior of ferromagnetic bilayers and how the super-exchange energy affects it. To this end, we compute, for several values of the super-exchange parameters, the final magnetization states of two configurations of bilayered ferromagnetic domains: one made of two stacked thin square plates and the other made of two stacked thin circular plates. We observe numerically the strong dependance of the final magnetization state with respect to the magnitude of the super-exchange energy.

1 Introduction

Ferromagnetic materials are of increasing importance in the industrial world. They have four main areas of applications: energy(transformers), furtivity, communications(wave circulators), data storage(hard drives), and nano electronic devices. In particular, heterogeneous media such as multilayers have been the subject of recent interest as these materials can exhibit behavior not observed in homogenous ferromagnetic media. For all these reasons, ferromagnetic materials have been the subject of many studies during the last decades. The literature concerning ferromagnetism is rather large, one may cite[1, 2, 3, 13] for an introduction on magnetism and ferromagnetism.

*Laboratoire Jean Kutzmann, Université de Grenoble

†Université Bordeaux, IMB, UMR 5251 CNRS, INRIA, F-33400 Talence, France. Kevin.Santugini@math.u-bordeaux1.fr

The magnetic behavior of ferromagnetic bodies depends heavily on their form. In particular, the presence of thin spacers in a ferromagnetic media can substantially modify their magnetic behavior. This is due not only to the change of geometry, but also to the apparition of new physical phenomena in-between the spacer: mainly super-exchange and surface anisotropy. Surface anisotropy penalizes the angle between the magnetization and the normal to the spacer. *I.E.*, surface anisotropy favors magnetizations that are parallel to the spacer on spacer's boundary. Super-exchange penalizes the jump of the magnetization across the spacer. *I.E.*, super-exchange favors magnetizations that do not jump across the spacer. See [8] for a much more detailed explanation of the involved physics. Results on the existence of solutions with surface energies may be found in [12, 9]. An asymptotic analysis on the behavior of massive ferromagnetic bodies split by a non magnetic spacer can be found in [10, 11]. In this paper, we do not consider surface anisotropy.

Our goal is to study the magnetic behavior of ferromagnetic bilayers made of two thin plates. Between the two layers lies a very thin spacer (much thinner than the plates themselves) made of a weakly magnetic material. If the spacer were to be made of void, there would be no super-exchange and only the demagnetization field would link the two layers. However, since the spacer is made of a weakly magnetic material, another energy, super-exchange, also links the two layers. The magnitude of the super-exchange interaction depends on both the thickness of the spacer and the material the spacer is made of. For an initial magnetization that is uniform in each layer and antiparallel across the two layers, we compute the final magnetization state. We consider two geometries of ferromagnetic bilayers: bilayers made of two square plates and bilayers made of two circular plates. We have the magnitude of the super-exchange vary and observe that whenever super-exchange dominates, the final state is the Landau configuration and whenever demagnetization field dominates, the final magnetization is mostly uniform in each layer and antiparallel across the layers. Between these two extreme, we observe several transition regimes. Identifying these regimes provides insight into the behavior of ferromagnetic bilayers.

In section 2, we remind the reader about the properties of ferromagnetic materials including one of its most common model: micromagnetism. Then, in section 3, we describe our numerical algorithms. Eventually, we present and analyze our numerical results in section 4 for square plates and in section 5 for circular plates.

2 Ferromagnetism and micromagnetism

Ferromagnetic materials can display a nonzero macroscopic magnetization even in the absence of any applied field. This sets them apart from weakly magnetic materials such as paramagnetic and diamagnetic materials. The magnetization of ferromagnetic media depends on all the past history of the applied field. This allows ferromagnetic materials to be used for data storage.

2.1 The micromagnetic model

The micromagnetic model is a possible model of ferromagnetism, see [2]. In this model, the magnetic state of a ferromagnetic material is characterized by a vector field: the magnetization $\boldsymbol{M}$. This magnetization is the average on the mesoscopic scale of the microscopic magnetization. Inside the ferromagnetic domain, the magnetization $\boldsymbol{M}$ has a constant norm M_s. It vanishes outside of the ferromagnetic domain.

The micromagnetic model assigns an energy E_p and a magnetic excitation $\boldsymbol{H}_p$ to each physical interaction p in a ferromagnetic media. The excitation are linked through the formula:

$$\mathrm{DE}(\boldsymbol{M}) \cdot (\boldsymbol{v}) = -\mu_0 \int_\Omega \boldsymbol{M} \cdot \boldsymbol{H}_p(\boldsymbol{M}) \mathrm{d}\boldsymbol{x}$$

The stationary state problem is completely characterized by the energies: the steady states of the magnetization are simply the local minimizers of the total energy. Usually, four main contributions to the total energy are considered

Exchange: Exchange is fundamental to ferromagnetic materials as it is responsible for the uniform magnetization at the mesoscopic scale. Without exchange, a ferromagnetic material would simply not be ferromagnetic. The exchange energy is given by:

$$\mathrm{E}_a(\boldsymbol{M}) = \frac{A^{\mathrm{phys}}}{2M_s^2} \int_\Omega \|\nabla \boldsymbol{M}\|^2 \mathrm{d}\boldsymbol{x}, \tag{1}$$

where $A^{\mathrm{phys}} > 0$ is the exchange parameter. Exchange penalizes the variations of the magnetization. At the microscopic level, exchange aligns the spins of neighboring electrons. Physicists explain exchange with quantum mechanics: it is due to the overlap of the electronic wave functions of neighboring atoms, see Aharoni [1, §3.2]. The associated magnetic excitation is $\boldsymbol{H}_e = A^{\mathrm{phys}}/(\mu_0 M_s^2) \triangle \boldsymbol{M}$.

Anisotropy: In many ferromagnetic materials, some directions of magnetizations are favored. This is due to the underlying crystallographic arrangement of these materials. One possible formula for the anisotropy energy is:

$$\mathrm{E}_a(\boldsymbol{M}) = \frac{1}{2M_s^2}\int_\Omega \left(\mathbf{K}^{\mathrm{phys}}(\boldsymbol{x})\boldsymbol{M}(\boldsymbol{x})\right)\cdot \boldsymbol{M}(\boldsymbol{x})\mathrm{d}\boldsymbol{x},$$

where $\mathbf{K}$ is a field of symmetric positive matrices. The contribution to the total excitation by anisotropy is $\boldsymbol{H}_a = -\mathbf{K}(\boldsymbol{x})\boldsymbol{M}(\boldsymbol{x})/(\mu_0 M_s^2)$.

Demagnetization field: It is the energy of the magnetic field:

$$\mathrm{E}_d(\boldsymbol{M}) = -\frac{\mu_0}{2}\int_\Omega \boldsymbol{M}(\boldsymbol{x})\cdot\boldsymbol{H}_d(\boldsymbol{x})\mathrm{d}\boldsymbol{x} = \frac{\mu_0}{2}\int_\Omega \|\boldsymbol{H}_d(\boldsymbol{x})\|^2\mathrm{d}\boldsymbol{x}. \tag{2}$$

where $\boldsymbol{H}_d$ is the solution in the sense of distribution in $\mathbb{R}^3$ of the magnetostatic equation

$$\mathrm{div}(\boldsymbol{M}+\boldsymbol{H}_d) = 0, \qquad \mathrm{curl}(\boldsymbol{H}_d) = 0.$$

Zeeman This is the energy applied by the external field

$$\mathrm{E}_z(\boldsymbol{M}) = -\mu_0\int_\Omega \boldsymbol{M}(\boldsymbol{x})\cdot\boldsymbol{H}_z(\boldsymbol{x})\mathrm{d}\boldsymbol{x},$$

where $\boldsymbol{H}_z$ is the applied field.

Throughout this paper, we only consider ferromagnetic bodies where only the exchange and the demagnetization field energies are present.

2.2 Surface energies: super-exchange

In the presence of spacers, other physical interactions may be involved. Among them, super-exchange and surface anisotropy may appear. Throughout this paper, we do not consider surface anisotropy. In the presence of thin spacers made of weakly magnetic materials, the super-exchange interaction may appear in the spacer, between the two ferromagnetic plates. Super-exchange penalizes the jump of the magnetization across the spacer. At the microscopic level, in quantum mechanics, super-exchange occurs between two ferromagnetic atoms when the electronic wave functions of both layers both overlap with an electronic wave function of the spacer, see Aharoni[1, §3.4]. This has two consequences. One, if the spacer is empty, *i.e.* made of void,

there can be no super-exchange. Second, for super-exchange to happen, the spacer must be no thicker than several atomic length.

In the micromagnetic model, super-exchange is modeled by a surface, see Labrune and Miltat[8]: energy:

$$\mathrm{E}_{se}^{\mathrm{phys}}(\boldsymbol{m}) = \frac{J_1^{\mathrm{phys}}}{M_s^2}\int_\Gamma \|\gamma^+\boldsymbol{M} - \gamma^-\boldsymbol{M}\|^2 \mathrm{d}\hat{\boldsymbol{x}} + \frac{J_2^{\mathrm{phys}}}{M_s^4}\int_\Gamma \|\gamma^+\boldsymbol{M}\wedge\gamma^-\boldsymbol{M}\|^2 \mathrm{d}\hat{\boldsymbol{x}},$$

where Γ is the spacer, γ^+ the trace application on one side of the spacer and γ^- the one on the other side of the spacer. In this paper, we do not consider the biquadratic term and set $J_2^{\mathrm{phys}} = 0\mathrm{J/m}^2$. We modify the value of J_1^{phys} between any two computation of the final magnetization state.

2.3 The Landau-Lifshitz equation

To predict the behavior in time of a ferromagnetic body, the micromagnetic model must be completed by a partial differential equation: the Landau-Lifshitz equation. The Landau-Lifshitz equation is given by:

$$\frac{\partial \boldsymbol{M}}{\partial t} = -g\mu_0(\boldsymbol{M}\wedge\boldsymbol{H} + \frac{\alpha}{M_s}\boldsymbol{M}\wedge(\boldsymbol{M}\wedge\boldsymbol{H})). \tag{3}$$

where $\boldsymbol{H}$ is the magnetic excitation, μ_0 the magnetic permeability of the void and g the gyromagnetic factor. To be complete, the Landau-Lifshitz PDE needs a boundary condition. Without surface energies, we would use the Neumann homogenous boundary condition. For the boundary condition, we choose the one satisfied by the stationary states of the magnetization, *i.e.* the surface component of the Euler-Lagrange condition on the total energy under the constraint $|\boldsymbol{M}| = M_s$ almost everywhere. When J_1^{phys} is non null and J_2^{phys} is null, the boundary condition on the exterior boundary is

$$\frac{A^{\mathrm{phys}}}{M_s^2}\frac{\partial \boldsymbol{M}}{\partial \boldsymbol{\nu}} = 0, \tag{4}$$

and, on the spacer, is:

$$\frac{A^{\mathrm{phys}}}{M_s^2}\frac{\partial \boldsymbol{M}}{\partial \boldsymbol{\nu}} = 2\frac{J_1^{\mathrm{phys}}}{M_s^2}\left(\gamma'\boldsymbol{M} - \frac{1}{M_s^2}(\gamma'\boldsymbol{M}\cdot\gamma\boldsymbol{M})\gamma\boldsymbol{M}\right), \tag{5}$$

where γ is the trace application on the spacer and γ' the trace application coming from the opposite side of the spacer. A more convincing justification for choosing that boundary condition is that it is the correct boundary condition to formally recover the following energy inequality:

$$\mathrm{E}_{\mathrm{tot}}(\boldsymbol{M}(\cdot,T)) + \frac{\alpha}{1+\alpha^2}\frac{1}{gM_s}\int_0^T \left\|\frac{\partial \boldsymbol{M}}{\partial t}\right\|_{L^2(\Omega)}^2 \mathrm{d}t \leq \mathrm{E}_{\mathrm{tot}}(\boldsymbol{M}(\cdot,0)),$$

where $\mathrm{E}_{\mathrm{tot}}$ is the total energy including the surface energies on the spacer.

2.4 Dimensionless system

It is often easier to work on a dimensionless system. The Landau-Lifshitz system can be made dimensionless by setting:

$$\boldsymbol{m} = \frac{\boldsymbol{M}}{M_s}, \qquad \boldsymbol{h} = \frac{\boldsymbol{H}}{M_s}, \qquad \mathrm{e}_p = \frac{\mathrm{E}}{\mu_0 M_s^2}, \qquad \hat{t} = g\mu_0 M_s t,$$
$$A = \frac{A^{\mathrm{phys}}}{\mu_0 M_s^2}, \qquad \mathbf{K} = \frac{\mathbf{K}^{\mathrm{phys}}}{\mu_0 M_s^2}, \qquad J_1 = \frac{J_1^{\mathrm{phys}}}{\mu_0 M_s^2}, \qquad J_2 = \frac{J_2^{\mathrm{phys}}}{\mu_0 M_s^2}.$$

The Landau-Lifshitz equation becomes:

$$\frac{\partial \boldsymbol{m}}{\partial \hat{t}} = -\boldsymbol{m} \wedge \boldsymbol{h} - \alpha \boldsymbol{m} \wedge (\boldsymbol{m} \wedge \boldsymbol{h}),$$

where $\boldsymbol{h} = A \triangle \boldsymbol{m} - \mathbf{K}\boldsymbol{m} + \boldsymbol{h}_d + \boldsymbol{h}_z$. The total energy becomes

$$\begin{aligned}\mathrm{e}_{\mathrm{tot}}(\boldsymbol{m}) = {} & \frac{A}{2}\int_\Omega \|\nabla \boldsymbol{m}(\boldsymbol{x})\|^2 \mathrm{d}\boldsymbol{x} + \frac{1}{2}\int_\Omega (\mathbf{K}(\boldsymbol{x})\boldsymbol{m}(\boldsymbol{x})|\boldsymbol{m}(\boldsymbol{x}))\mathrm{d}\boldsymbol{x} \\ & + \frac{1}{2}\int_\Omega \|h_d(\boldsymbol{x})\|^2 \mathrm{d}\boldsymbol{x} - \int_\Omega h_z(\boldsymbol{x})\boldsymbol{m}(\boldsymbol{x})\mathrm{d}\boldsymbol{x} + J_1 \int_\Gamma \|\gamma^+\boldsymbol{m} - \gamma^-\boldsymbol{m}\|^2 \mathrm{d}\hat{\boldsymbol{x}}.\end{aligned}$$

And the boundary condition (5) on the spacer becomes

$$A\frac{\partial \boldsymbol{m}}{\partial \boldsymbol{\nu}} = 2J_1\left(\gamma'\boldsymbol{m} - (\gamma'\boldsymbol{m}\cdot\gamma\boldsymbol{m})\gamma\boldsymbol{m}\right). \tag{6}$$

Numerically, we solve the dimensionless system. However, the value of the parameters usually found in the literature are the physical values and not the dimensionless ones. It is important to know the usual normalization of these physical parameters and how to compute the dimensionless parameters from the physical ones.

3 Discretization and algorithms

To compute the steady states of bilayers, we use the dynamic equation and iterate in time till convergence. With this method, we obtain the final state of the magnetization given a particular initial condition instead of the global minimizer. To realize this computation, we discretize in time and space the Landau-Lifshitz system. All the computation is done in the dimensionless system.

Name	Symbol	Value	Unit
Exchange	A^{phys}	10^{-11}	J/m
Saturated Magnetization	M_s	1.4×10^6	A/m
Anisotropy	$\mathbf{K}^{\text{phys}}$	$\mathbf{0}$	J/m^3
Dissipation parameter	α	0.5	Dimensionless

Table 1: The ferromagnetic parameters of Permalloy in `SI`

To discretize in space, we use a finite volume discretization with a regular node centered cubic mesh. For non rectangular geometries, we simply apply a mask over a rectangle containing the considered domain. This choice allows us to compute the demagnetization field operator using Toeplitz matrices and the Fast Fourier Transform, see S. Labbé and P. Leca [4, 6, 7]. The anisotropy term is local and easily discretized by averaging $\mathbf{K}^{\text{phys}}$ over each cell of the mesh. The exchange term is computed via the standard seven points stencil. To discretize the nonlinear Neumann boundary condition, the discretized exchange term must be modified near the boundary. This is done via the fictitious point method: in the seven point stencils. When computing the exchange at $(i, j, 1)$, the values of the discretized magnetization at $(i, j, 2)$ are replaced using the discretized version of (6), see [Equation (6.2)][11].

As in [4, 6], the Landau-Lifshitz equation is discretized in time by a second order scheme:

$$\begin{aligned} \boldsymbol{m}_{k+1} - \boldsymbol{m}_k &= \delta t_k \boldsymbol{F}(\boldsymbol{m}_k) + \frac{\delta {t_k}^2}{2} \mathrm{D}\boldsymbol{F}(\boldsymbol{m}_k) \cdot \boldsymbol{F}(\boldsymbol{m}_k), \\ \boldsymbol{F}(\boldsymbol{m}_k) &= -\boldsymbol{m}_k \wedge \boldsymbol{h}(\boldsymbol{m}_k) - \alpha \boldsymbol{m}_k \wedge (\boldsymbol{m}_k \wedge \boldsymbol{h}(\boldsymbol{m}_k)). \end{aligned}$$

where $\boldsymbol{m}_k$ is the magnetization at time t_k and $\delta t_k = t_{k+1} - t_k$. The time step size δt_k is is chosen at each step so as to maximize energy loss, see [4, 6, 5].

4 Steady states for square plates

4.1 Geometry

We consider two square plates as drawn in figure 1. Each plate is made of the same material: permalloy. Each plate is a square 294.4 nanometers wide. The ferromagnetic parameters of permalloy in the `SI` system are given in Table 1.

For our numerical experiments, we set $J_2^{\text{phys}} = 0\text{J/m}^2$ and have J_1^{phys} vary between 10^{-6}J/m^2 and $8 \times 10^{-4}\text{J/m}^2$.

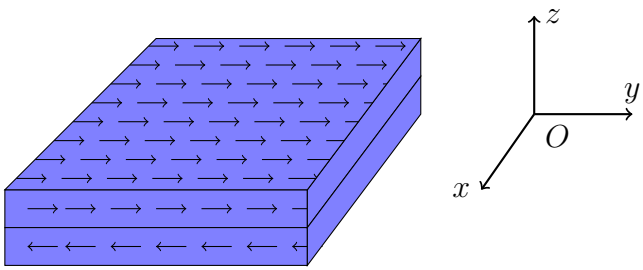

Figure 1: The square bilayer initial magnetization

The meshing is a regular $128 \times 128 \times 2$ meshing. The mesh stepsize $h = 2.3$ nanometers and each square plate is 294.4 nanometers wide.

We perform the simulations for several different values of the J_1^{phys} parameter. The initial magnetization $\boldsymbol{m}$ is uniform $(0, 1, 0)$ in the upper plate and uniform $(0, -1, 0)$ in the lower plate.

4.2 Numerical results

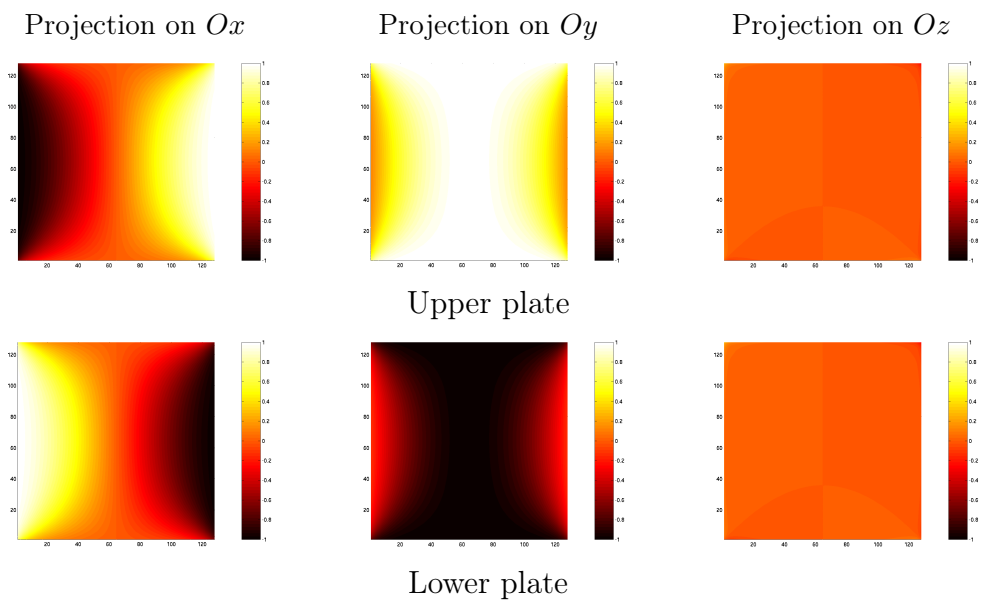

Figure 2: Numerical result: Square plates, Steady state: $\boldsymbol{m}$, $J_1^{\text{phys}} = 3.5 \times 10^{-5}\text{J/m}^2$

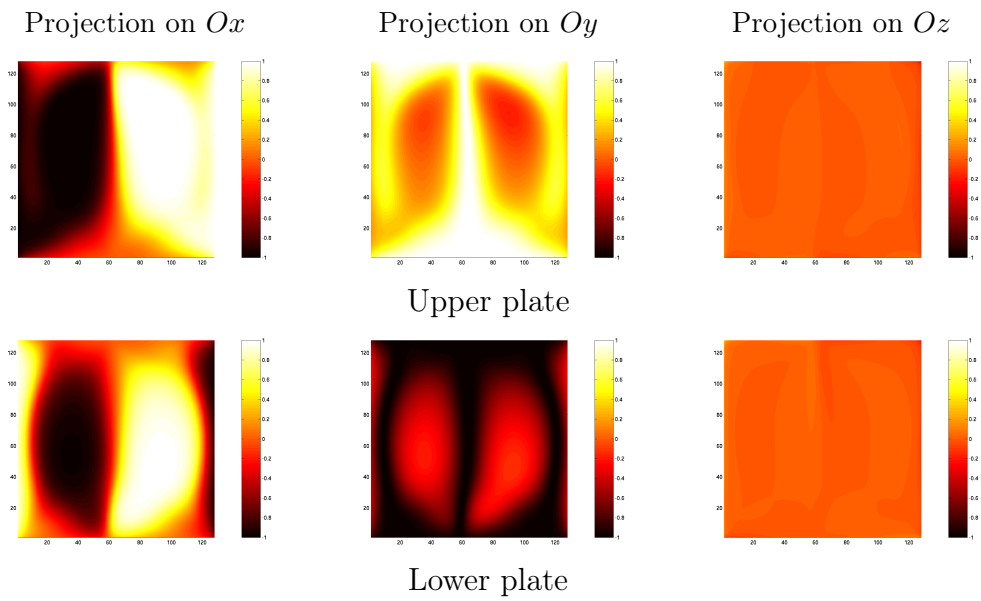

Figure 3: Numerical result: Square plates, Steady state:$\boldsymbol{m}$, $J_1^{\text{phys}} = 5 \times 10^{-5}\text{J/m}^2$

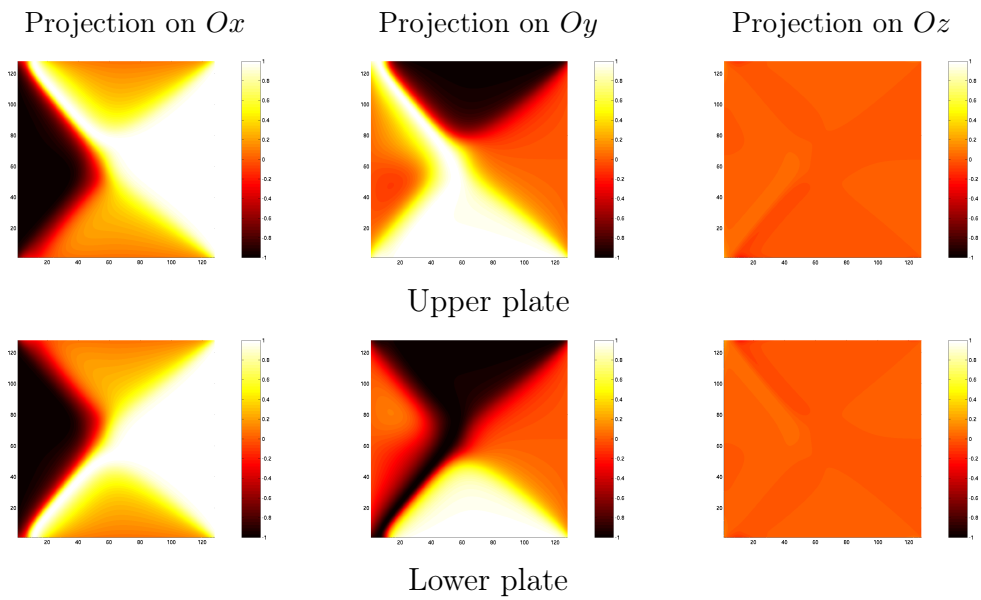

Figure 4: Numerical result: Square plates, Steady state: $\boldsymbol{m}$, $J_1^{\text{phys}} = 6 \times 10^{-5}\text{J/m}^2$

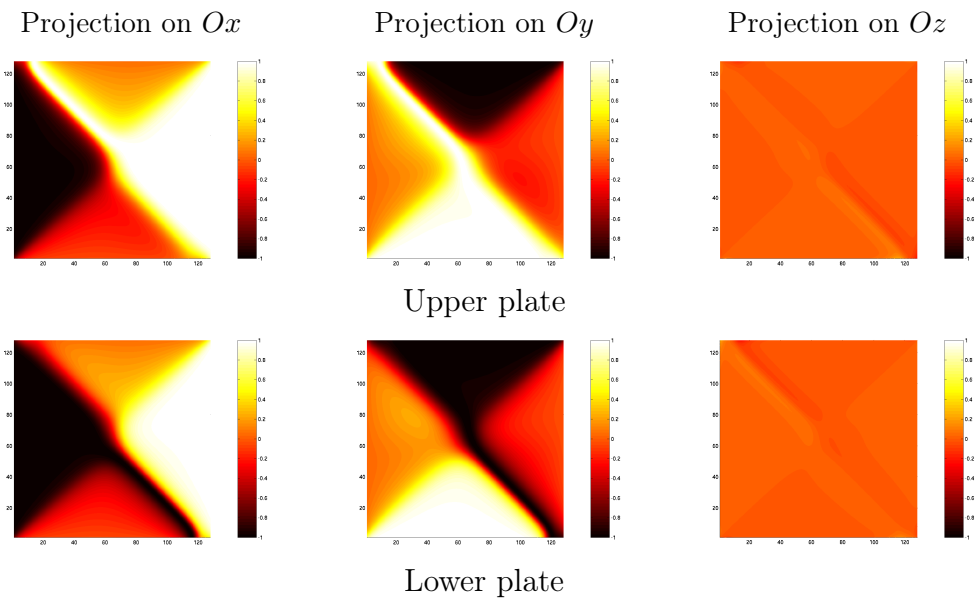

Figure 5: Numerical result: Square plates, Steady state, $\boldsymbol{m}$, $J_1^{\text{phys}} = 9 \times 10^{-5}\text{J/m}^2$

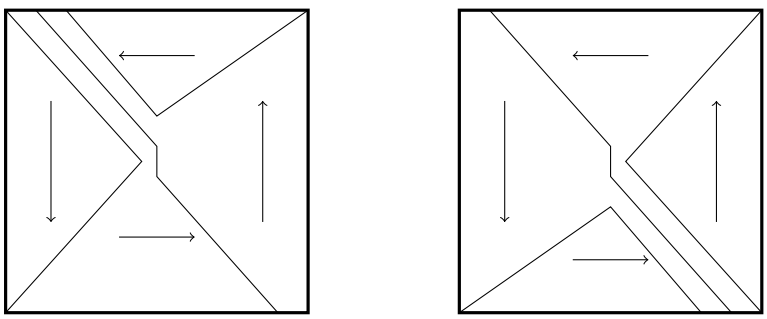

Figure 6: Schematic representation: square plates, steady state $J_1^{\text{phys}} = 9 \times 10^{-5}\text{J/m}^2$

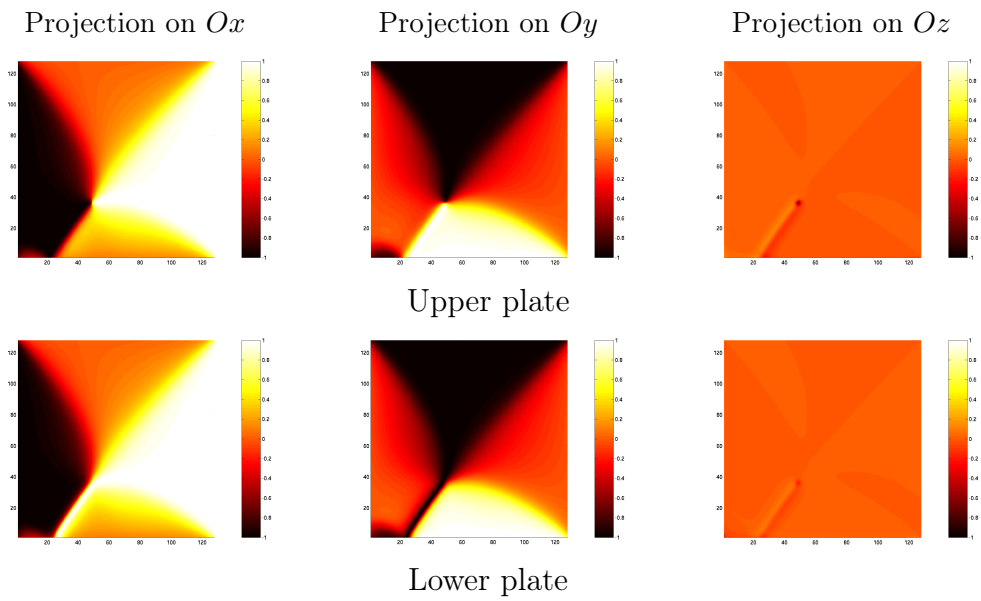

Figure 7: Numerical result: Square plates, Steady state: $\boldsymbol{m}$, $J_1^{\text{phys}} = 5 \times 10^{-4}\text{J/m}^2$

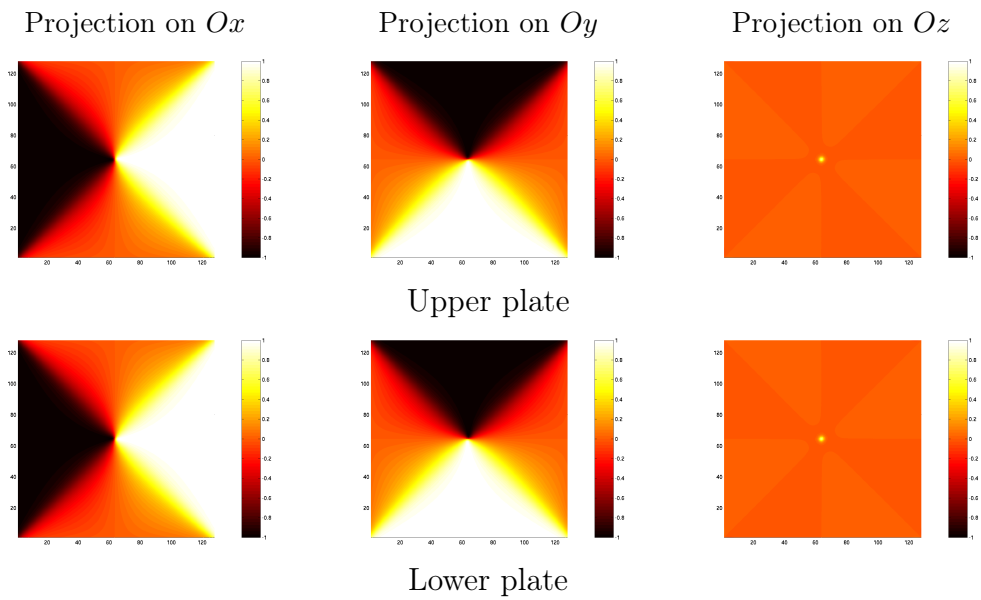

Figure 8: Numerical result: Square plates, Steady state: $\boldsymbol{m}$, $J_1^{\text{phys}} = 6 \times 10^{-4}\text{J/m}^2$

Lowest computed J/m^2	**Highest computed** J/m^2	**Qualitative steady state**
0	3.5×10^{-5}	Almost uniform magnetization, Figure 2.
4×10^{-5}	5×10^{-5}	U-shaped configuration, Figure 3.
5.5×10^{-5}	2×10^{-4}	Almost Landau configuration with fast unfolding on a semi diagonal in both plates, Figures 4 and 5.
2.5×10^{-4}	5.5×10^{-4}	Decentered Landau configuration on one plate, almost decentered Landau configuration with fast unfolding on the other plate, Figure 7.
6×10^{-4}	8×10^{-4}	Identical Landau configuration in both plates, Figure 8.

Table 2: Dependance of the final steady states on J_1^{phys} in square bilayers

For square plates, we have computed the final state of the magnetization for 27 different values of the super-exchange parameter J_1^{phys} ranging from 0J/m^2 to 8×10^{-4}J/m^2. We have identified 5 different configurations, see Table 2. The four main ones are: uniform, U-shaped, almost Landau and Landau. The other one is an hybrid with one main configuration on one plate and another one in the other plate. As super-exchange strengthens, the jump of the magnetization between the plates diminishes. We present one or two numerical results per configuration. These results are presented in false colors. The colors represent the magnitude of the x (first column), y (second column) or z(third column) coordinate of the dimensionless magnetization $\boldsymbol{m}$. Please note that here, x is directed upward and y is directed rightward.

Let's comment on the final state of the magnetization when $J_1^{\text{phys}} = 3.5 \times 10^{-5}$J/m^2, see Figure 2 where the results are presented in false colors. Super exchange is dominated by the demagnetization field and we get a steady state when the magnetization is uniform in each plate. In the upper plate, the magnetization $\boldsymbol{m}$ is mostly uniformly equal to $(0, 1, 0)$ and in the lower plate mostly uniformly equal to $(0, -1, 0)$. Only close to the boundary of the square does the magnetization detract from these values. The jump of the magnetization when one goes from the lower to the upper plate is big. This is to be expected considering the low magnitude of super-exchange in that case.

When $J_1^{\text{phys}} = 5 \times 10^{-5}\text{J/m}^2$, super-exchange is stronger and the magnetization doesn't jump as much between the two plates, see Figure 3. In each plate we observe a U-shaped configuration. The magnetization between the two plates jumps only near the boundary of the square. There is practically no jump of the magnetization between the two plates in the interior of the square.

If we increase the magnitude of the super-exchange interaction and have $J_1^{\text{phys}} = 6 \times 10^{-5}\text{J/m}^2$ or $J_1^{\text{phys}} = 9 \times 10^{-5}\text{J/m}^2$, we observe a completely different state of the magnetization, see Figures 4 and 5. In each plate this configuration looks almost like the Landau configuration where the magnetization circles in the direct sense around the center of the plate. However on one of the four semi diagonal, the magnetization unfolds very rapidly in the indirect sense on a very small distance. See Figure 6 for a schematic representation of how magnetization unfolds in the final steady state when $J_1^{\text{phys}} = 9 \times 10^{-5}\text{J/m}^2$. If the semi diagonals where the unfolding occurs are opposite in the lower and upper plate, then the vortex is centered. If the semi diagonals are adjacent, then the vortex is pulled toward the common side of both of these semi diagonals. This happens because fast unfolding is costly in both exchange and super-exchange energy so it is advantageous to limit the length of the semi diagonals on which fast unfolding occurs. Note that in this configuration, there is no vortex at the center of the "vortex".

If the super-exchange parameter J_1^{phys} increases to $5 \times 10^{-4}\text{J/m}^2$, then the magnetization takes a Landau configuration in the upper plate but keeps the almost Landau configuration with fast unfolding in the lower plate, see Figure 7. However the vortex is not centered. This is due to the high cost in exchange and super-exchange energy of the unfolding. Since there is only one semi diagonal where it happens, it minimizes energy by limiting the length of the semi diagonal where magnetization unfolds and pulling the center of the almost vortex toward the bottom left.

Finally, when the magnitude of super-exchange is high enough, for example with $J_1^{\text{phys}} = 6 \times 10^{-4}\text{J/m}^2$, we recover the Landau configuration, see Figure 8. In the discrete formulation, super-exchange of high enough magnitude, when $J_1^{\text{phys}} = A^{\text{phys}}/(2h)$, is equivalent to no spacer between the two plates. Therefore, it is unsurprising we recover the final steady state obtained[1] in the absence of a spacer, *i.e.* the Landau configuration, when super-exchange dominates.

[1]We verified that known result using our program. However, the Landau configuration obtained with a no spacer geometry is indistiguishable to the naked eye from the Landau configuration obtained with super-exchange interaction of a strong enough magnitude. Hence, we chose not to include the false color representation of the magnetization for the no spacer case

5 Steady states for circular plates

5.1 Geometry

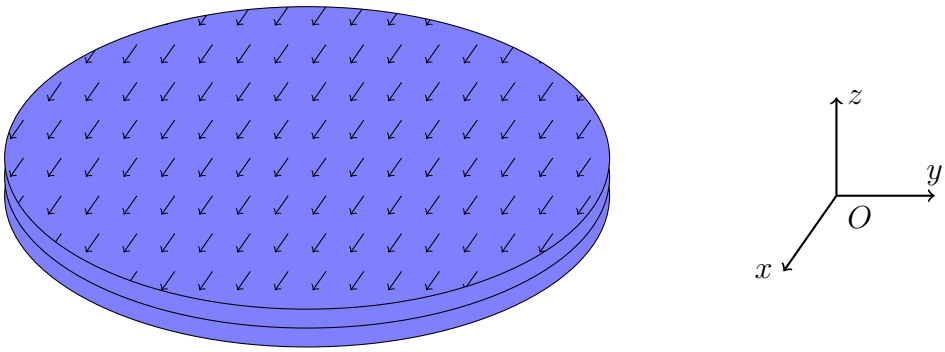

Figure 9: The circular bilayer initial magnetization, reversed in lower plate

We consider two circular plates as drawn in figure 9. Each plate is made of the same material: permalloy. Each plate is a circular plate whose diameter is 294 nanometers. The ferromagnetic parameters of permalloy in the `SI` system are given in Table 1. For our numerical experiments, we set $J_2^{\text{phys}} = 0\text{J/m}^2$ and have J_1^{phys} vary between 10^{-6}J/m^2 and $8 \cdot 10^{-4}\text{J/m}^2$.

The meshing is a regular $128 \times 128 \times 2$ meshing. The mesh stepsize $h = 2.3$ nanometers and each circular plate is 296 nanometers wide along its diameter.

We perform the simulations for several different values of the J_1^{phys} parameter. The initial magnetization $\boldsymbol{m}$ is uniform $(-1, 0, 0)$ in the upper plate and uniform $(1, 0, 0)$ in the lower plate.

5.2 Numerical results

For circular plates, we have computed the final state of magnetization for 28 values of the super-exchange parameter J_1^{phys} ranging from 0J/m^2 to $8 \times 10^{-4}\text{J/m}^2$. We have identified 5 different configurations, see Table 3. The four main one are quasi-uniform, almost Landau, U-shaped, and Landau. The other is a double vortex Landau configuration. These different regimes aren't as frozen in circular bilayers as they are with square bilayers: the same configuration may appear multiple time rotated by various angles in the case of circular bilayers. The difference in behavior compared to square bilayers is mainly due to the smooth boundary without corners in circular bilayers.

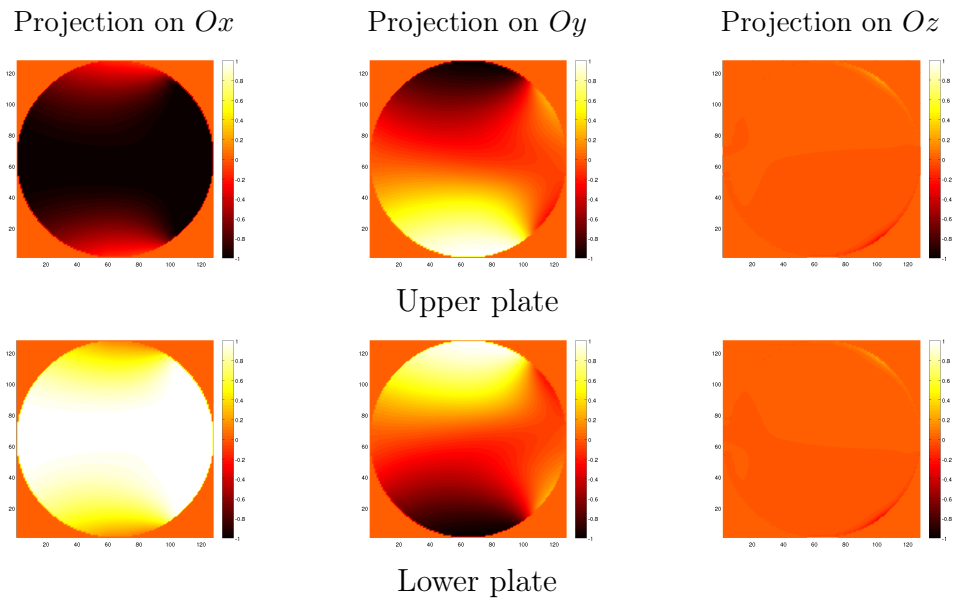

Figure 10: Numerical result: Circular plates, Steady state: $\boldsymbol{m}$, $J_1^{\text{phys}} = 4 \times 10^{-5}\text{J/m}^2$

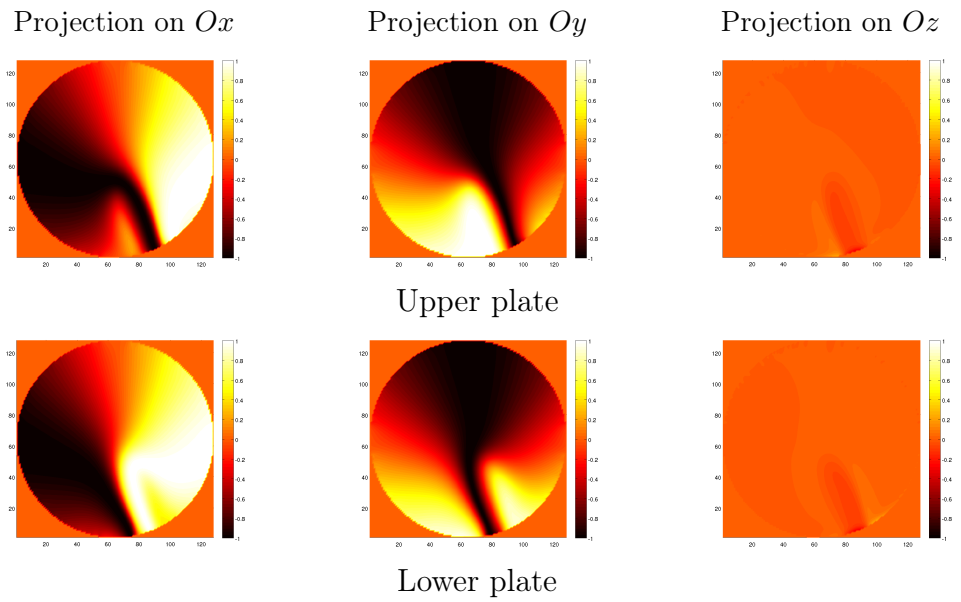

Figure 11: Numerical result: Circular plates, Steady state: $\boldsymbol{m}$, $J_1^{\text{phys}} = 6 \times 10^{-5}\text{J/m}^2$

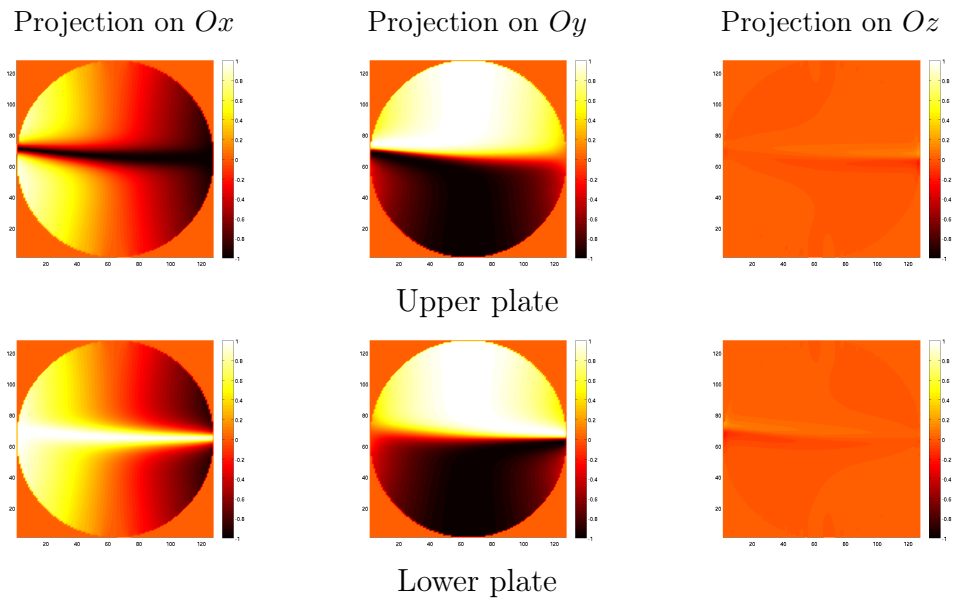

Figure 12: Numerical result: Circular plates, Steady state: $\boldsymbol{m}$, $J_1^{\text{phys}} = 1.5 \times 10^{-4}\text{J/m}^2$

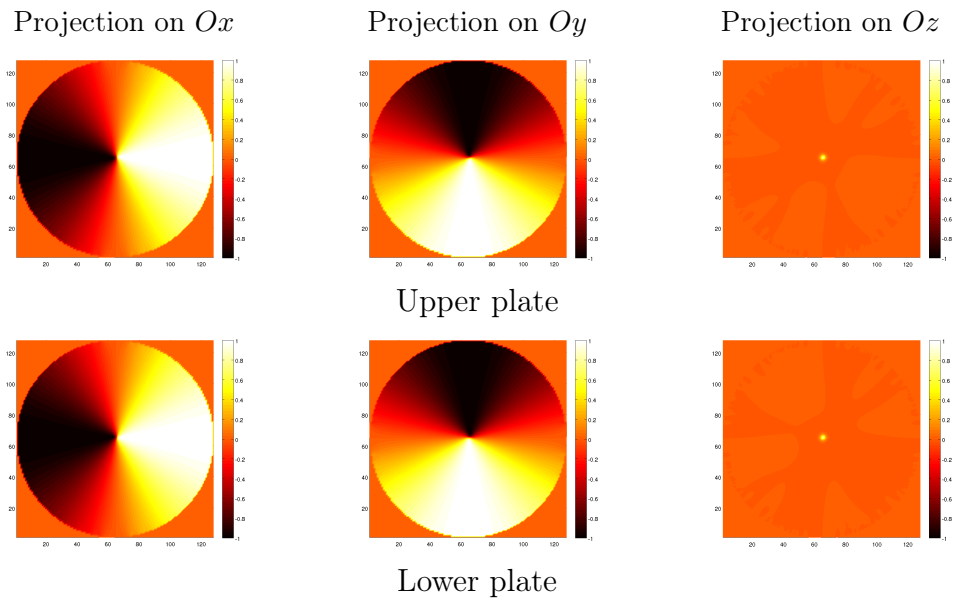

Figure 13: Numerical result: Circular plates, Steady state: $\boldsymbol{m}$, $J_1^{\text{phys}} = 4 \times 10^{-4}\text{J/m}^2$

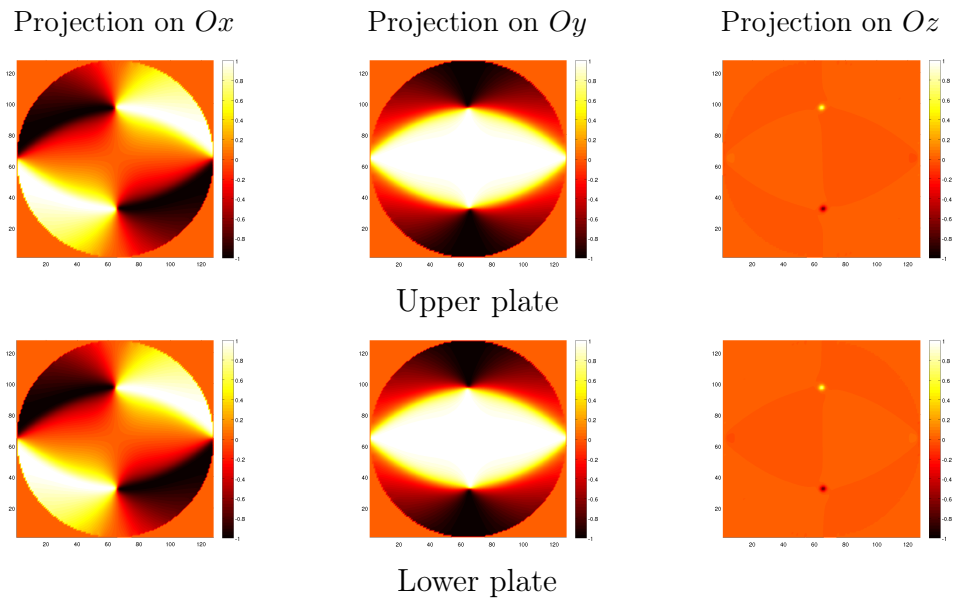

Figure 14: Numerical result: Circular plates, Steady state: $\boldsymbol{m}$, $J_1^{\text{phys}} = 4.5 \times 10^{-4}\text{J/m}^2$

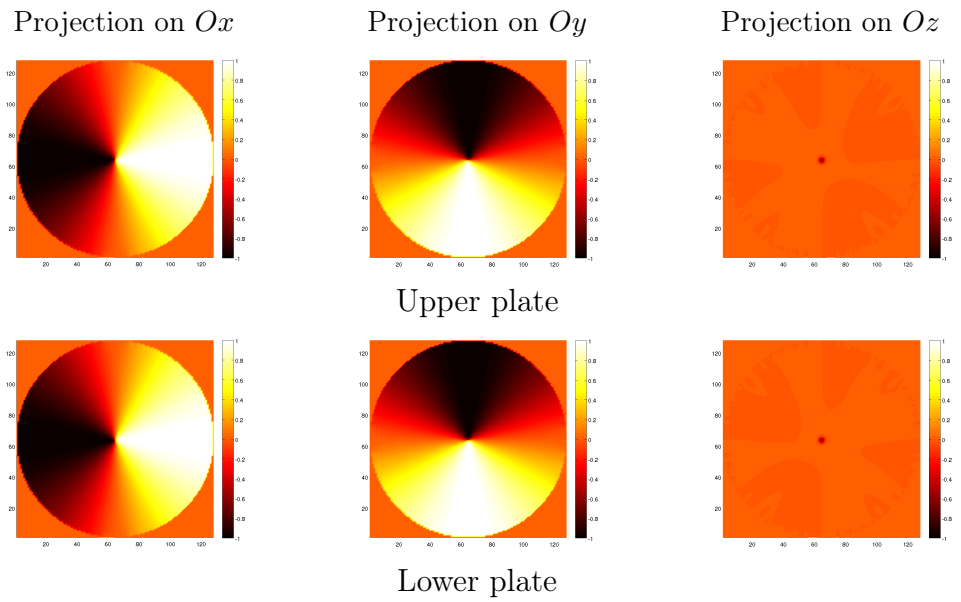

Figure 15: Numerical result: Circular plates, Steady state: $\boldsymbol{m}$, $J_1^{\text{phys}} = 5 \times 10^{-4}\text{J/m}^2$

Lowest computed J/m^2	**Highest computed** J/m^2	**Qualitative steady state**
0	4×10^{-5}	Almost uniform magnetization, Figure 10.
5×10^{-5}	7.5×10^{-5}	Almost Landau configuration with fast unfolding on one radius of the circular plate, Figure 11.
8×10^{-5}	2.5×10^{-4}	U-shaped configuration, Figure 12.
3×10^{-4}	8×10^{-4}	Identical Landau configuration in both plates,Figures 13 and 15 , double vortex for special value $J_1^{\text{phys}} = 4.5 \times 10^{-4}$, Figure 14.

Table 3: Dependance of the final steady states on J_1^{phys} in circular bilayers

In non smooth domains such as square, the corners permit the apparition of low energies singularities.

When the super-exchange parameter J_1^{phys} is lower than 4×10^{-5}J/m^2, we observe a quasi uniform magnetization in each plate. In the upper plate, the magnetization $\boldsymbol{m}$ is mostly uniformly equal to $(-1, 0, 0)$ and in the lower plate mostly uniformly equal to $(1, 0, 0)$, see Figure 10. The magnetization reverses across the spacer. The super-exchange interaction is dominated by the demagnetization interaction and cannot force the alignment of the magnetization across the spacer.

For higher values of the super-exchange parameter J_1, when $J_1^{\text{phys}} = 6 \times 10^{-5}$J/m^2 ,we observe an almost Landau configuration. In that configuration, magnetization unfolds along one radius of each circular plate. Super-exchange is strong enough to prevent magnetization from jumping across the spacer in the vast majority of the circular plates. The only place where magnetization jumps between the lower and the upper plate is in the small part of the plates where the unfolding happens.

For even higher values of the super-exchange parameter, when J_1^{phys}, $J_1^{\text{phys}} = 6 \times 10^{-5}$J/m^2, we observe a U-shaped configuration, see Figure 12. The magnetization looks like a U rotated 90 degrees couterclockwise in the upperplate, and clockwise in the lower plate. In that configuration, magnetization unfolds along one diameter of each circular plate. Super-exchange is strong enough to prevent magnetization from jumping across the spacer in the vast majority of the plates except where the horizontal diameter of each

circular plate is located.

When the super-exchange parameter J_1^{phys} is greater than $4 \times 10^{-4}\text{J/m}^2$, the steady state of the magnetization is none other than the Landau configuration, see Figures 13 and 15. However, for $J_1^{\text{phys}} = 4.5 \times 10^{-4}\text{J/m}^2$, we instead observe a double vortex instead of a singular one, see Figure 14.

6 Conclusion and future work

To increase our understanding in how super-exchange affects the magnetization in bilayers, we computed the final steady state for bilayers while changing the value of one super-exchange parameter in between every two simulation.. For square bilayers, we identified five different regimes of the magnetization in bilayers depending on the magnitude of the super-exchange interaction and see how the final state of the magnetization changes from an antiparallalel, almost uniform in each plate, magnetization to the Landau configuration when super-exchange strengthens. For circular bilayers, we also identified five regimes, but for circular bilayers, the different regimes aren't as different as those exhibited by square bilayers.

We only kept and represented the final steady state of the magnetization, it would also be interesting to observe how the magnetization evolves from the initial uniform antiparallel state to the final steady state in each of these different regimes. In particular, it would be interesting to know how long it takes for the magnetization to reach the steady state and see how this time depend on the magnitude of the super-exchange. More geometries could also be considered: trilayers, quadrilayers, imbricated spheres or imbricated cylinders.

It would be extremely interesting to compute the microwave susceptibility of such ferromagnetic object in order to predict their behavior in terms of energetic restitution. The first application of such a study stands in the radar protection where the goal is to give back the energy possible in the detectable frequencies. The second application would be devoted to the magnetic detection, in particular, the response of collections of well chosen magnetic dots could be a very efficient tools in order to analyze the frequencies of tenuous magnetic signals.

References

[1] A. Aharoni. *Introduction to the theory of ferromagnetism.* Oxford Science Publication, 1996.

[2] W.F. Brown. *Micromagnetics.* Interscience Publishers, 1963.

[3] L. Halpern and S. Labbé. La théorie du micromagnétisme. Modélisation et simulation du comportement des matériaux magnétiques. *Matapli*, 66:77–92, September 2001.

[4] S. Labbé. *Simulation numérique du comportement hyperfréquence des matériaux ferromagnétiques.* PhD thesis, Université Paris 13, Décembre 1998.

[5] S. Labbé and P.Y. Bertin. Microwave polarisability of ferrite particles with non-uniform magnetization. *Journal of Magnetism and Magnetic Materials*, 206:93–105, 1999.

[6] S. Labbé and P. Leca. Résolution rapide des équations de Maxwell quasistationnaires : matrices Toeplitz multidimensionnelles. Application au micromagnétisme. *C. R. Acad. Sci. Paris*, Série I(t. 327):415–420, 1998.

[7] Stéphane Labbé. Fast computation for large magnetostatic systems adapted for micromagnetism. *SISC SIAM J. on Sci. Comp.*, 26(6):2160–2175, 2005.

[8] M. Labrune and J. Miltat. Wall structure in ferro / antiferromagnetic exchange-coupled bilayers : a numerical micromagnetic approach. *Journal of Magnetism and Magnetic Materials*, 151:231–245, 1995.

[9] K. Santugini-Repiquet. *Matériaux ferromagnetiques: influence d'un espaceur mince non magnétique, et homogénéisation d'agencements multicouches, en présence de couplage sur la frontière.* Thèse de doctorat, Université Paris 13, Villetaneuse, dec 2004.

[10] K. Santugini-Repiquet. Modelization of a split in a ferromagnetic body by an equivalent boundary condition: Part 1. the classical case: no surface energies present. *Asymptotic Analysis*, 47(3–4):227–259, 2006.

[11] K. Santugini-Repiquet. Modelization of a split in a ferromagnetic body by an equivalent boundary condition: Part 2. the influence of super-exchange and surface anisotropy. *Asymptotic Analysis*, 47(3–4):261–290, 2006.

[12] K. Santugini-Repiquet. Solutions to the Landau-Lifshitz system with nonhomogenous Neumann boundary conditions arising from surface anisotropy and super-exchange interactions in a ferromagnetic media. *Nonlinear Anal.*, 65(1):129–158, July 2006.

[13] É. Trémolet de Lacheisserie, editor. *Magnétisme: Fondements*, volume I of *Collection Grenoble Sciences*. EDP Sciences, 2000.